

Mineralogic investigation of Capri/Ganges/Eos Chasmata, Mars: Insights into the geologic history of Valles Marineris. J. Flahaut¹, C. Quantin¹, J. L. Bishop², F. Fueten³, P. Allemand¹, N. Mangold⁴, F. Poulet⁵ and J-P. Bibring⁵. ¹LGL/CNRS, UCBL/ENS Lyon, 2 rue Raphaël Dubois, 696222 Villeurbanne Cedex, France (jessica.flahaut@ens-lyon.org). ²SETI Institute/NASA-ARC, Mountain View, CA, 94043. ³Department of Earth Sciences, Brock University, St. Catharines, Ontario, Canada. ⁴LPGN/CNRS, Université Nantes, France. ⁵IAS, CNRS/Université Paris-Sud, Orsay, France.

Valles Marineris represents a unique vertical section through the uppermost kilometers of the martian crust. Its location, east of Tharsis bulge, and its water-related history suggest a great diversity of rock types in this area. We present here detailed analyses of Ganges, Capri and Eos chasmata using high resolution morphologic and mineralogic data from the Mars Reconnaissance Orbiter (MRO) mission.

Introduction: Valles Marineris has been studied mostly for its water-related morphologies and its important past aqueous activity [1,2]. Multiple flow features appear to erode out of the kilometer-thick interior layered deposits (ILDs) that are found in most of its canyons [3]. Recent surveys suggest that these ILDs are sulfate-rich Hesperian deposits that likely filled the canyon voids after their formation [4,5,6]. Sulfates have also been detected in association with hydrated silica in layered deposits draped over the Hesperian plateaus around the western end of Valles Marineris (Juventae, Ius, Melas and Ganges Chasmata) [7,8]. The hydrated mineralogy of the area is even more diverse since clays were also observed on the surrounding Noachian plateaus and in the upper section of the walls of the eastern outlet canyons, namely Coprates, Capri and Ganges Chasmata [9]. Finally, the area has also been recently suggested to be a key place to observe older, mafic-rich pristine Noachian material, such as crustal outcrops exposed in the deepest canyon walls [10].

The present study investigates the area of Ganges, Capri and Eos chasmata, located in the eastern end of Valles Marineris, and at the beginning of the outflow channels that extend eastward (fig. 1a). These chasmata have not yet been well studied, although they exhibit a unique combination of mineralogies and remarkable deposits. They also expose terrains of various ages, ranging from the late Noachian (southern plateaus) to the early Amazonian (canyon floor), or even older through their walls (fig 1b).

Regional context: Capri, Eos, and Ganges Chasmata form trough systems interconnected to the east with the chaotic terrains and outflow channels of the southern circum-Chryse region of Mars [11]. They all present so-called chaotic floors, which are typically attributed to voluminous emanations of fluids and associated ground collapse during the Late Hesperian

Epoch. A few hundreds kilometers wide, all of these chasmata have an average floor elevation of around -4000 m, whereas the surrounding plateaus peak between -700 m to the east and +2000 m to the west.

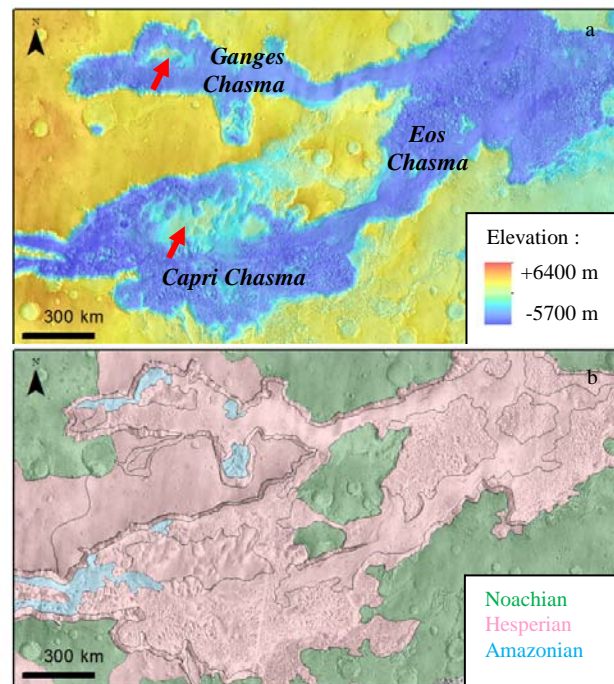


Figure 1: a- View of the study area on a MOLA topographic map overlaid on a THEMIS IR day global mosaic. The red arrows point out the locations of the main kilometer-thick ILDs. b- Age distribution, based on the geologic map of [12].

Datasets: A Geographic Information System (GIS) was built to gather data from different Martian missions. Themis Visible and Infrared day and night data from the Mars Odyssey Spacecraft were used, in association with the Mars Orbiter Camera (MOC) data from the Mars Global Surveyor mission, and the High Resolution Imaging Science Experiment (HiRiSE) and Context Camera (CTX) data from the MRO mission. A Mars Orbiter Laser Altimeter (MOLA) elevation map of 300 m per pixel was added to this image collection, providing topographic data. This combination of images offers full spatial coverage of the study area. Hyperspectral and multispectral data from the Compact Reconnaissance Imaging Spectrometer for Mars

(CRISM) on board MRO were used to determine mineralogical composition. CRISM is providing images at 544 different wavelengths (at 6.55 $\mu\text{m}/\text{channel}$) between 0.362 and 3.92 μm in hyperspectral mode, compared to 72 wavelengths in multispectral mode. Spatial resolutions range from 18 to 40 m per pixel for hyperspectral data to 100 to 200 m per pixel for multispectral ones. All the data have been corrected for atmospheric contribution and georeferenced. The atmosphere is removed using a ratio with a CRISM scene of Olympus Mons, scaled to the same column density of CO_2 as in [13]. We processed mineralogical maps from atmospherically corrected CRISM data that we then projected over HiRiSE and CTX data in our GIS.

Results: Mafic minerals. Mafic minerals were identified by broad absorptions in the Visible Near Infrared (VNIR) domain, which are due to the electronic transition of Fe^{2+} in octahedral coordination [14]. Olivine was detected thanks to its broad and strong absorption between 0.8 and 1.5 μm , around the ILDs of Ganges Chasma, the outlet of the chasma, and on most of Eos Chasma's floor (dark blue spectrum, fig. 2). CRISM spectra do not enable assignment of a unique olivine type so far, but multiple geologic contexts seem present. Pyroxenes were also identified on the floor and within the canyon walls, by the presence of two coupled absorptions in the 1 μm and in the 2 μm domains (cyan spectrum, fig. 2). The short-wavelength band centers of the rocky outcrops (around 0.9 and 1.8 μm) suggest the presence of Low-Calcium Pyroxenes (LCP) such as enstatite [10] whereas High-Calcium Pyroxenes (HCP) typically have longer-wavelength band centers (1.05 and 2.3 μm) and are more often present in association with sand.

Sulfates Sulfate minerals were identified by a characteristic 2.4 μm feature that is indicative of the SO_4 vibrations in the molecule structure. Both polyhydrated (PHS) and monohydrated (MHS) sulfates are detected, with additional absorption bands at 1.9 μm for polyhydrated sulfates, and 2.1 μm for monohydrated sulfates [4,6,15] (orange and red spectra, fig. 2). These detections correspond mostly to the massive interior layered deposits within Ganges and Capri Chasmata, although some signatures are present elsewhere within the canyons.

Hydrated Silicates Clays of various types are identified with narrow absorptions near 1.4, 1.9, and 2.2 or 2.3 μm , depending on their cationic compositions [16]. Fe/Mg-rich phyllosilicates with absorptions at 1.4, 1.9, and 2.31 μm , consistent with a mixture of saponite and putative chlorite, are observed within the walls of Valles Marineris [10] (dark green spectrum,

fig. 2). More surficial clay-rich deposits are observed on the plateaus surrounding the study area, and consist of a mixture of Fe/Mg-rich phyllosilicates (*e.g.*, nontronite) and Al-rich phyllosilicates (*e.g.*, montmorillonite) [9]. Opaline Silica might be present locally within the canyon [17].

Conclusion and perspectives: Valles Marineris exhibits a diverse mineralogy through terrains of variable ages. The geologic contexts are under study for the spectral units described here. The results will be used to present an extended geologic history for the Valles Marineris region and discuss potential climatic implications.

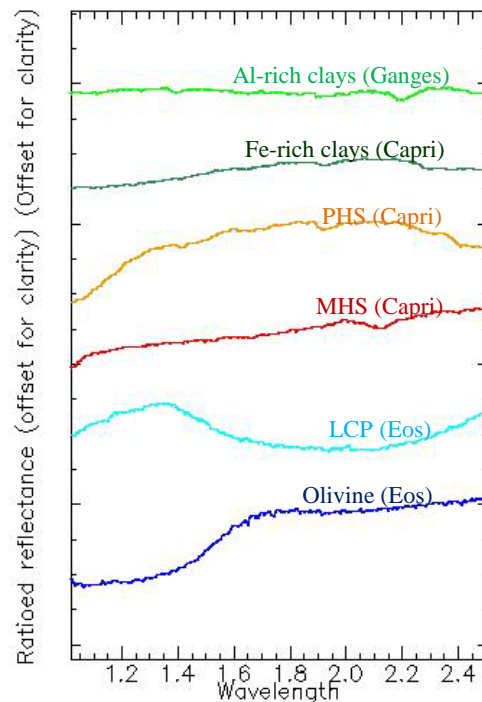


Figure 2: CRISM spectra of the minerals that were most commonly detected within the study area.

References: [1] Carr M. (1996) *Oxford*. [2] Baker V.R. (1982) *University of Texas Press*. [3] Lucchitta B. et al. (1994) *JGR*, 99. [4] Gendrin A. et al. (2005), *Science*, 307. [5] Quantin C. et al. (2005), *LPSC 36th*, #1789. [6] Mangold N. et al. (2008), *JGR*, 113(E8). [7] Weitz C. et al. (2009), *Icarus*, 205. [8] Le Deit L. et al. (2010), *Icarus*, 208. [9] Le Deit L. et al. (2012) *accepted to JGR*. [10] Flahaut J. et al. (2012), *Icarus*, in press. [11] Sharp R.P., 1973, *JGR*, 78. [12] Scott D.H. and K.L. Tanaka (1986), *U.S. Geol. Surv. Misc. Invest.* [13] Murchie S.L. et al. (2009), *JGR*, 114. [14] Burns R.G. (1993), *Cambridge University Press*. [15] Bishop J.L. et al. (2009), *JGR*, 114. [16] Bishop J.L. et al. (2008), *Clay Minerals*, 43. [17] Flahaut J. et al. (2010), *JGR*, 115.